We are IntechOpen, the world's leading publisher of Open Access books Built by scientists, for scientists

4,800
Open access books available

122,000
International authors and editors

135M
Downloads

Our authors are among the

154
Countries delivered to

TOP 1%
most cited scientists

12.2%
Contributors from top 500 universities

WEB OF SCIENCE™

Selection of our books indexed in the Book Citation Index in Web of Science™ Core Collection (BKCI)

Interested in publishing with us?
Contact book.department@intechopen.com

Numbers displayed above are based on latest data collected.
For more information visit www.intechopen.com

12

Numerical Simulation of Plasma Kinetics in Low-Pressure Discharge in Mixtures of Helium and Xenon with Iodine Vapours

Anatolii Shchedrin and Anna Kalyuzhnaya
Institute of Physics, National Academy of Sciences of Ukraine
Ukraine

1. Introduction

Due to ecological problems related to the utilization of gas-discharge ultraviolet (UV) mercury vapour lamps widely used in lighting technology, photochemistry, and photomedicine, there arises a need for developing new mercury-free sources of UV radiation using electron bands of rare-gas monohalides and halogen molecules as well as spectral lines of their atoms (Lomaev et al., 2003). The most high-power mercury-free lamps are UV emitters with "chlorine - noble gas" active media emitting on transitions of the excimer molecules XeCl (308 nm) and KrCl (222 nm). The use of aggressive chlorine molecules in the gas mixtures of such emitters results in a comparatively low mixture life (1-100 hours), which impedes their wide application in various optical technologies. It is mainly due to the absorption of chlorine by open metal electrodes (especially strongly heated cathode) and its heterophase chemical reaction with a quartz discharge tube accompanied by the formation of polymer compounds (chlorosiloxanes).

That is why the replacement of chlorine molecules by less aggressive iodine ones in the working media of excilamps represents an urgent task. Ultraviolet radiation of glow discharge plasma in mixtures of helium with iodine vapours that is still transparent to air is mainly concentrated in the spectral ranges 175-210 nm and 320-360 nm. The mixture life of such lamps reaches 10^3 hours (Lomaev & Tarasenko, 2002; Shuaibov et al., 2005a, 2005b). The use of the He-Xe-I_2 active medium in a glow discharge lamp also allows one to obtain emission of the excimer molecule XeI(B-X) (253 nm) (Shuaibov, 2004 et al.). Moreover, of special interest is the fact that the wavelength of this transition is close to that of the most intense spectral line of the mercury atom in low-pressure gas-discharge lamps, which is used in a number of optical technologies. The basic spectral lines of the iodine atom (183.0, 184.5, 187.6, and 206.2 nm) (Liuti & Mentall, 1968) are also close to those of the mercury atom (184.9, 194.2, 202.7, and 205.3 nm) now used in the corresponding low pressure UV emitters.

In this connection, it is important to optimize output characteristics of helium-iodine and xenon-iodine gas discharge emitters. The kinetics of plasmachemical processes in the gas discharge plasma in mixtures of noble gases with iodine molecules was till now studied only for high-pressure emitters excited by a barrier discharge (BD) in krypton-iodine and xenon-iodine mixtures (Zhang & Boyd, 1998, 2000). The conditions of BD plasmachemical

reactions that lead to the formation of excited iodine atoms and molecules as well as xenon iodide molecules differ substantially from those in a longitudinal low-pressure glow discharge. Therefore, the results of these calculations cannot be used to analyze the efficiency and physics of the processes taking place in excimer glow discharge lamps. The parameters and kinetics of plasmachemical processes in low-pressure plasma in mixtures of noble gases with iodine vapors were not studied till now.

In order to optimize the output characteristics of gas-discharge lamps based on helium-iodine and xenon-iodine mixtures, we have carried out numerical simulation of plasma kinetics in a low-pressure discharge in the mentioned active media. This chapter reports on systematic studies of the electron-kinetic coefficients in mixtures of helium and xenon with iodine vapors as well as in the He:Xe:I_2 mixture. The mean electron energies and drift velocities in the discharge are calculated. A comparative analysis of the distributions of the power introduced into the discharge between the dominant electron processes in helium-iodine and xenon-iodine mixtures is performed. The rates of electron-molecular processes were computed based on the numerical solution of the Boltzmann equation in the two-term approximation that provides a good description of the electron energy distribution function in the case where the electron thermal velocity considerably exceeds the drift one (which is true in all experiments).

The plasma kinetics in the active medium of the excimer UV emitter was numerically simulated by solving a system of kinetic equations for neutral, excited, and charged components together with the Boltzmann equation for the electron energy distribution function and the supply circuit equation. The kinetic model used in the calculation included more than 60 elementary processes. The simulation of the plasma kinetics allowed us to obtain the relation between the emission intensities of atomic and molecular iodine in the helium-iodine mixture as well as to analyze the effect of xenon on the relation between the emission intensities of iodine atoms and molecules as well as xenon iodide molecules in the mixture including xenon.

Based on the analysis of plasmachemical processes running in the active medium of the helium-iodine excimer lamp, we studied the dependences of the emission intensities of atomic and molecular iodine on the total pressure of the mixture and revealed the basic mechanisms of the pressure influence on the population kinetics of the emitting levels. The effect of the halogen concentration on the emission intensity of atomic and molecular iodine is investigated and the main factors resulting in the decrease of the emission intensity with varying halogen content are found.

The performed numerical simulation yielded good agreement with experiment, which first of all testifies to the right choice of the calculation model and elementary processes for numerical simulation.

2. Numerical simulation

2.1 Electron energy distribution function

The electron energy distribution function is of major importance for understanding processes running in the active medium of a gas discharge. It determines parameters significant for the analysis of the plasma kinetics, such as rates of elementary electron-impact processes in the discharge, mean electron energy and mobility. In the case of not too strong fields, where the thermal electron velocity considerably exceeds their drift velocity, the distribution function can be expanded in terms of the parameter characterizing its

anisotropy. Restricting oneself to two terms of such an expansion and considering elastic and inelastic collisions of electrons with neutral particles, one arrives at the Boltzmann equation in the two-term approximation (Golant, 1980):

$$\frac{1}{n_e N}\sqrt{\frac{m}{2e}}\varepsilon 1/2\,\frac{\partial(n_e f)}{\partial t}-\frac{1}{3}\left(\frac{E}{N}\right)^2\frac{\partial}{\partial\varepsilon}\left(\frac{\varepsilon}{\sum_i \frac{N_i}{N}Q_{Ti}}\frac{\partial f}{\partial\varepsilon}\right)-\frac{\partial}{\partial\varepsilon}\left[2\sum_i\frac{N_i}{N}\frac{m}{M_i}Q_{Ti}\varepsilon^2\left(f+T\frac{\partial f}{\partial\varepsilon}\right)\right]=S_{eN}. \quad (1)$$

Here, f stands for the symmetric part of the electron energy distribution function, ε, n_e, and m and the electron energy, density, and mass, correspondingly, E is the electric field in the discharge, T denotes the gas temperature (eV), N is the total gas concentration, N_i, M_i, and Q_{Ti} are the concentrations of atoms or molecules, their masses and momentum-transfer cross sections, and e=1.602·10^{-12} Erg/eV. The function $f(\varepsilon)$ is normalized by the condition

$$\int_0^\infty \varepsilon^{1/2} f(\varepsilon)\,d\varepsilon = 1. \quad (2)$$

The integral S_{eN} describing inelastic electron collisions with atoms and molecules has the form

$$S_{eN}=\sum_i\frac{N_j}{N}\left[\left(\varepsilon+\varepsilon_i\right)Q_i\left(\varepsilon+\varepsilon_i\right)f\left(\varepsilon+\varepsilon_i\right)-\varepsilon Q_i(\varepsilon)f_0(\varepsilon)\right]-\frac{N_{at}}{N}\varepsilon Q_{at}(\varepsilon)f(\varepsilon), \quad (3)$$

where Q_i and ε_i denote the cross sections and energy thresholds of the processes of electron-impact excitation, ionization, or dissociation of neutral species, correspondingly, while Q_{at} is the cross section for electron attachment to electronegative molecules.

The solution of Eq.(1) was obtained using the Thomas algorithm for tridiagonal matrices. Electron-electron collisions were not taken into account when calculating the distribution function due to the fact that their effect on the electron distribution at low electron densities ($n_e/N > 10^{-6}$) is negligible (Soloshenko et al., 2007).

A considerable part of iodine molecules in a gas discharge dissociates into atoms (Barnes & Kushner, 1998). That is why the Boltzmann equation for the electron energy distribution function was solved under the assumption that the halogen component in the discharge is presented by I_2 molecules (50%) and I atoms (50%) in the ground state.

One of the difficulties accompanying numerical modeling of the plasma kinetics in iodine-containing mixtures is the absence of both experimental and theoretical data on electron-impact excitation cross sections of iodine molecules. This fact is confirmed, in particular, by the bibliographic study of data on electron collisions with halogen molecules published in the 20th century performed by the National Institute for Fusion Science (Hayashi, 2003). That is why it is now generally accepted to allow for these processes using approximations of various kinds. For example, in (Avdeev et al., 2007), where the authors investigated the kinetics in the krypton-iodine mixture, the cross sections for inelastic electron collisions with iodine molecules were approximated based on general theories described in (Smirnov, 1967). In (Boichenko & Yakovlenko, 2003), the rates of electron-impact excitation and step

ionization of iodine molecules were assumed to be the same as the corresponding rates for its atoms.

The solution of the Boltzmann equation and the simulation of the plasma kinetics in the active medium of an UV emitter were carried out with regard for three excited levels of the iodine molecule. As will be shown below, they play the key role in the formation of emitting iodine atoms and molecules. The excitation cross sections for these levels were introduced as those similar to the excitation cross section of the emitting state of the iodine atom shifted by the excitation threshold for each specific level of the iodine molecule. The cross section for electron dissociative attachment to iodine molecules was taken from (Tam & Wong, 1978), whereas the cross sections of the other electron collisions with iodine atoms and molecules were analogous to those used in (Avdeev et al., 2007). The processes of electron interactions with noble gas atoms are well studied. The cross sections for elastic and inelastic electron collisions with helium atoms are presented in (Rejoub et al., 2002; Saha, 1989; Cartwright & et al., 1992) and those with xenon atoms can be found in (Rejoub et al., 2002; NIFS; Hyman, 1979).

Knowing the electron energy distribution function, it is possible to analyze the distribution of the power introduced into the discharge among the most important electron processes. As was shown in (Soloshenko, 2009), the power spent for an electron-impact inelastic process with the threshold energy ε_{ei} can be presented as

$$W_{ei} = \sqrt{\frac{2e}{m}} n_e N_i \varepsilon_i \int_0^\infty \varepsilon Q_{ei}(\varepsilon) f(\varepsilon) d\varepsilon \,, \tag{4}$$

where Q_{ei} is the cross section of the corresponding inelastic process. The power spent for gas heating is described by the relation

$$W_i = \frac{2m}{M_i} \sqrt{\frac{2e}{m}} n_e N_i \int_0^\infty \varepsilon^2 Q_{Ti}(\varepsilon) f(\varepsilon) d\varepsilon \,, \tag{5}$$

where Q_{Ti} is the momentum-transfer cross section for electron scattering by atoms and molecules of the mixture. So, the specific power spent for an electron process has the form

$$\eta_i = \frac{W_{ei}}{\sum_j W_{ej} + \sum_j W_j}. \tag{6}$$

2.1 Plasma kinetics in mixtures of helium and xenon with iodine vapours

The time evolution of the concentrations of neutral, charged, and excited particles in the active medium of the excimer UV emitter was found by solving the system of kinetic equations

$$\frac{dN_i}{dt} = \sum_{ij} k_{ij} N_j + \sum_{ijl} k_{ijl} N_j N_l + \dots \,, \tag{7}$$

where N_i are the concentrations of the corresponding components of the mixture and k_{ij}, k_{ijl} are the rates of kinetic reactions. In this case, the rates of inelastic electron-impact processes

represent variable quantities due to their dependence on the electron energy distribution function:

$$k_{ie} = \sqrt{\frac{2e}{m}} \int_0^\infty \varepsilon Q_i(\varepsilon) f(\varepsilon) d\varepsilon. \tag{8}$$

In turn, the electron energy distribution is determined by the electric field in the discharge. That is why the construction of a self-consistent model of kinetic processes in the excimer-lamp medium requires the joint solution of the supply circuit equation, the Boltzmann equation, and the system of kinetic equations for the components of the medium.

The plasma kinetics was calculated for an excimer lamp operating on the helium-iodine and xenon-iodine mixtures as well as the ternary helium-xenon-iodine mixture in the pressure range 1-10 Torr. The diagram of the experimental set-up whose parameters were used for the numerical simulation will be given in what follows. It was assumed that the UV emitter is supplied by a constant voltage circuit with the ballast resistance R_b=10^4 Ohm and the charging voltage U_0=6 kV. The discharge resistance represents a variable quantity depending on the electron density in the discharge n_e and their mobility μ:

$$R = \frac{1}{\sigma}\frac{d}{S} = \frac{1}{en_e\mu_e}\frac{d}{S}, \tag{9}$$

where σ stands for the conductivity of the active medium, d is the interelectrode distance, and S is the electrode area.

The emission of UV lamps based on helium-iodine mixtures includes a spectral line corresponding to the electron transition of iodine atoms with a wavelength of 206 nm and the $I_2(D' \rightarrow A')$ molecular band with a wavelength of 342 nm. The diagram of the energy levels of atomic and molecular iodine is presented in Fig.1 (Barnes & Kushner, 1996). Solid lines mark the states taken into account in the described kinetic model.

It was already noted that, due to the absence of experimental or theoretical data on electron excitation cross sections of iodine molecules, they were introduced as those of the emitting state of the iodine atom shifted by the excitation threshold for each specific level of the I_2^* molecule. The effect of the inaccuracy in the values of these cross sections was estimated by means of test calculations of the plasma kinetics with the use of the cross sections twice larger and lower than those accepted in the kinetic model. It was found out that the variation of the excitation cross section of the $I_2(D)$ state does not considerably influence the emission power of both atomic and molecular iodine – their change is less than 1%. The variation of the excitation cross section of the $I_2(D')$ level results in the 8% and 35% change of the emission powers of atomic and molecular iodine, correspondingly. In the case of variation of the excitation cross section of the $I_2(B)$ level, the emission powers of atomic and molecular iodine change by 35% and 13%, correspondingly. Such a result is acceptable with regard for the fact that the general behavior of the theoretical curves did not change in the case of variation of the cross sections.

Molecular iodine effectively dissociates into atoms due to a number of elementary processes. Its recovery to the molecular state takes place at the walls of the discharge chamber (Barnes & Kushner, 1998). That is why the kinetic model takes into account the diffusion of iodine atoms to the walls. For this purpose, we include an additional process of conversion of atomic iodine to the molecular form taking place with the rate equal to the diffusion loss frequency of iodine atoms. The diffusion loss frequency was estimated as D/Λ^2 (Raizer,

1991), where D is the diffusion coefficient and Λ is the characteristic length scale. For a discharge tube representing a long cylinder with radius r_0, $\Lambda = r_0/2.4$ (Raizer, 1991). The diffusion coefficient in the mixture He-I_2 = 130-130 Pa was taken equal to 100 cm^2/s. In the case of variation of the quantitative composition of the active medium, the diffusion coefficient changed proportionally to the mean free path of iodine atoms in the mixture.

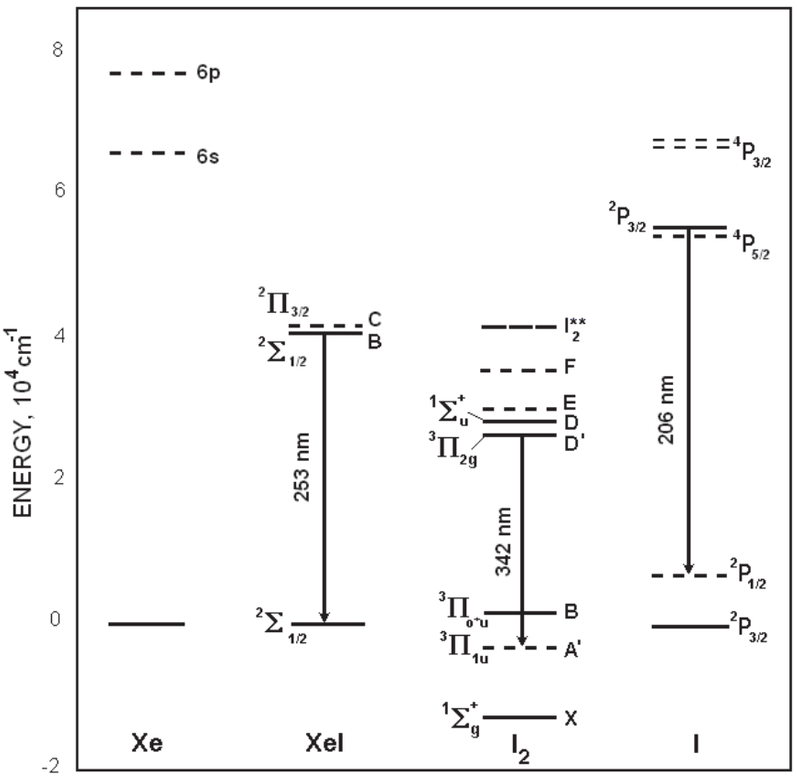

Fig. 1. Energy level diagram in the UV emitter

The full set of reactions used for the simulation of the plasma kinetics in the mixture of helium with iodine vapours is presented in Table 1 (Shuaibov et al., 2010a). As was already noted, the rates of electron-impact processes 1-11 were calculated at every time moment from the electron energy distribution function. The rates of ion-ion recombination (reactions 24-25) were calculated as functions of the pressure according to the Flannery formulas (McDaniel & Nighan, 1982). The rates of the other reactions used in the kinetic scheme were taken from (Avdeev et al., 2007; Boichenko & Yakovlenko, 2003; Kireev & Shnyrev, 1998; Stoilov, 1978; Baginskii et al., 1988).

The addition of xenon to the active medium of a helium-iodine UV-emitter results in the appearance of an additional radiation band at 253 nm corresponding to the B→X transition of XeI* excimers (Fig.1). Excimer molecules of rare gas halides (RX*) are generated in the discharge due to two basic algorithms. One of them is the ion-ion recombination ($R^+ + X^-$) that runs in the presence of a third body and is therefore of minor importance under the used low-pressure conditions and the other is the so-called harpoon reaction between an excited rare gas atom and a halogen molecule ($R^* + X_2$). However, as was shown by detailed studies (Barnes & Kushner, 1996, 1998), the harpoon reaction does not play a significant role

in the formation of XeI* excimers. The main channel of their generation at pressures ≤ 5 Torr is the reverse harpoon reaction between a xenon atom in the ground state and a highly excited I_2** levels. The specific iodine levels participating in the reverse harpoon process were not identified. Nevertheless, it is clear that neither of the states considered in our kinetic scheme has enough energy to provide the excitation of the XeI* molecule.

№	Reaction	Rate, cm^6/s, cm^3/s, s
1	e+He > He*+e	Calculated from the Boltzmann equation
2	e+He > He^++e+e	
3	e+I_2 > I_2(B)+e	
4	e+I_2 > I_2(D)+e	
5	e+I_2 > I_2(D′)+e	
6	e+I_2 > I_2^++e+e	
7	e+I_2 > I^-+I	
8	e+I_2 > I+I+e	
9	e+I > I*+e	
10	e+I > I^++e+e	
11	e+I* > I^++e+e	
12	I_2(B)+He > I+I+He	1.0e-11
13	I_2(D)+He > I_2(D′)+He	1.0e-12
14	I_2(D)+I_2 > I_2(D′)+I_2	1.5e-11
15	I_2(D)+I > I_2(D′)+I	1.5e-11
16	I_2(D)> I_2+hv	1.6e-8
17	I_2(D′)+He > I_2 +He	1.0e-12
18	I_2(D′)+ I_2 > I_2 + I_2	1.0e-11
19	I_2(D′)+I > I_2 +I	1.0e-11
20	I_2(D′)> I_2+hv (342 nm)	7.0e-9
21	I* > I + hv (206 nm)	3.5e-9
22	I+I+M > I_2+M	3.0e-33
23	I*+I_2 > I_2(D)+I	1.3e-9
24	I^++I^-+M > I_2(D′)+M	Calculated by the Flannery formulas
25	I_2^++I^-+M > I_2(D′)+I+M	
26	He*+2He > He_2*+He	4.3e-34
27	He^++2He > He_2^++He	8.0e-32
28	He*+He* > He^++He+e	2.0e-10
29	He_2*+He_2* > He_2^++2He+e	5.0e-10
30	He_2* > He+He	3.6e8
31	He_2*+e > He+He+e	3.8e-9
32	He_2^++e > He+He	1.3e-11
33	2I > I_2	k_{diff}

Table 1. Kinetic reactions in the He-I_2 mixture

Thus, there are no ideas about both the levels of molecular iodine whose excitation contributes to the formation of XeI* and the rate of the reverse harpoon reaction. That is why, when calculating the kinetics in the He:Xe:I_2 medium, we introduced an additional excited level I_2** with the energy sufficient to excite the XeI molecule that took part in the reverse harpoon reaction (Fig. 1). Its rate was taken equal to the characteristic rate of the harpoon reaction (1.0e-9 cm^3/s) (Rhodes, 1979), whereas the excitation cross section of the I_2** level was chosen so that to provide the fraction of emission in the XeI*(B→X) band close to the experimental one. Such an approach allows us to analyze the effect of xenon on the emission intensities of atomic and molecular iodine. The set of reactions with participation of xenon is listed in Table 2. The used literature sources were the same as in Table 1.
Numerical simulation of the plasma kinetics in mixtures of helium and xenon with iodine vapours allowed us to obtain the relation between the emission intensities of iodine atoms and molecules, to calculate their dependences on the buffer gas pressure and halogen concentration, and to analyze the effect of xenon on the emission intensity of the medium.

3. Results of numerical simulation

3.1 Electron energy distribution function and electron-kinetic coefficients

Figure 2 presents the electron energy distribution functions calculated in the He-I_2-I= 800-50-50 Pa and Xe-I_2-I= 800-50-50 Pa mixtures at various values of the reduced electric field in the discharge E/N (50-300 Td) (Shuaibov et al., 2009).

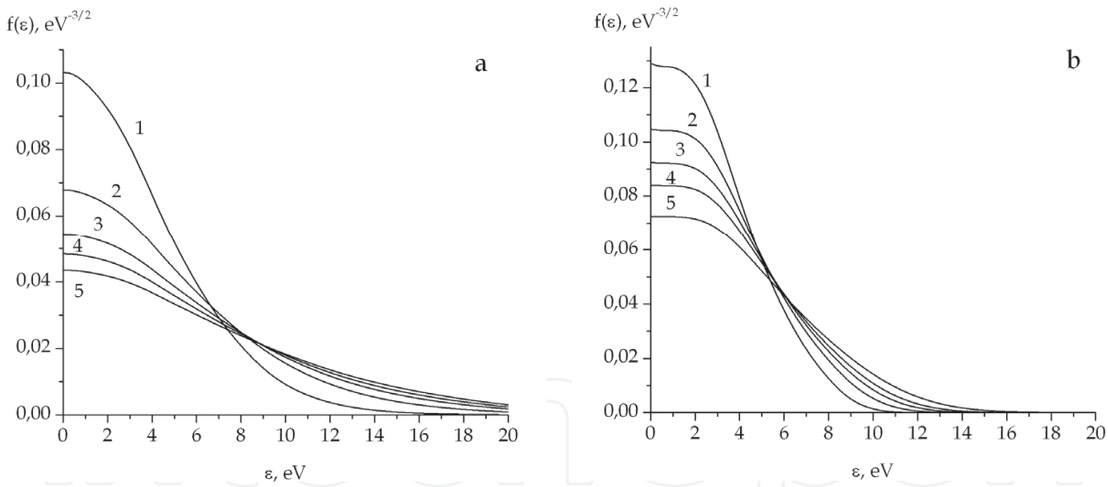

Fig. 2. Electron energy distribution functions calculated in the He-I_2-I= 800-50-50 Pa (a) and Xe-I_2-I= 800-50-50 Pa (b) mixtures at E/N = 50 (1), 100 (2), 150 (3), 200 (4), and 300 (5) Td

One can see that the replacement of the helium buffer gas by xenon results in the decrease of the portion of high-energy electrons in the discharge. It is due to the fact that the excitation and ionization thresholds of xenon atoms (8.3 eV and 12.1 eV, correspondingly) are significantly lower than those of helium (19.8 eV and 22.5 eV), therefore the tail of the distribution function in the xenon mixture is cut off at lower energies.
The drift velocities and the mean electron energies calculated as functions of the electric field in the discharge in the studied mixtures are shown in Fig.3 (Shuaibov et al., 2009). One can see that the increase of the reduced field from 50 to 300 Td results in the linear growth of the drift

№	Reaction	Rate, cm^6/s, cm^3/s, s
1	e+Xe > Xe*+e	Calculated from the Boltzmann equation
2	e+Xe > Xe^++e+e	
3	e+Xe* > Xe^++e+e	
4	e+ I_2 > I_2**+e	
5	I_2(B)+Xe > I+I+Xe	2.0e-10
6	I_2(D)+Xe > I_2(D')+Xe	6.0e-12
7	I_2(D')+Xe > I_2+Xe	1.0e-12
8	I_2**+He > I_2+He	1.0e-12
9	I_2**+ I_2> I_2+ I_2	1.0e-12
10	I_2**+I > I_2+I	1.0e-12
11	I_2**+Xe > XeI*+ I	1.0e-10
12	Xe^++ I^-+M > XeI*+M	4.0e-26
13	XeI*+ I_2 > Xe+ I_2+I	5.0e-10
14	XeI*+Xe > Xe+Xe+I	9.2e-12
15	XeI* > Xe+I+hv (253 nm)	1/1.2e-8
16	Xe^++Xe > Xe_2^+	1.0e-31
17	Xe_2^++e > Xe*+Xe	2.44e-7
18	Xe_2^++e > Xe^++Xe+e	2.44e-7
19	Xe*+I > Xe+ I*	1.0e-10
20	Xe_2*+I > Xe+Xe+ I*	1.0e-10
21	XeI*+I_2 > Xe + 3I	1.0e-9
22	Xe^++He+Xe > Xe_2^++He	1.3e-31
23	Xe^++Xe+Xe > Xe_2^++Xe	3.6e-31
24	He^++He+Xe > He_2^++Xe	1.1e-31
25	Xe*+Xe* > Xe+ Xe^++e	5.0e-10
26	Xe*+Xe* > Xe_2^++e	1.1e-9
27	He*+Xe > Xe^++He+e	7.5e-11
28	He^++Xe > Xe^++He	1.0e-11
29	Xe*+Xe+Xe > Xe_2*+Xe	8.0e-32
30	Xe*+Xe+He > Xe_2*+He	1.4e-32
32	Xe_2*> Xe+Xe	6.0e7
33	Xe_2*+ I_2> Xe+Xe+ I_2(D')	2.0e-10
34	Xe*+ I_2> Xe+ I_2(D')	2.0e-10
35	2I > I_2	k_{diff}

Table 2. Kinetic reactions with participation of xenon in the He-Xe-I_2 mixture

velocity in the He-I_2-I medium in the range 10^7 – $5 \cdot 10^7$ cm/s, while in the Xe-I_2-I discharge, it changes in the interval $2 \cdot 10^6$ – $8 \cdot 10^6$ cm/s. In this case, the mean electron energy increases from 5.3 to 8.8 eV (He-I_2-I mixture) and from 4.2 to 7.5 eV (Xe-I_2-I mixture). The highest mean energies are observed in the helium medium characterized by a pronounced high-energy tail of the electron energy distribution function. The replacement of helium by xenon results in the abrupt cut-off the electron distribution at energies close to the xenon excitation threshold and, correspondingly, reduction of the mean electron energy in the discharge.

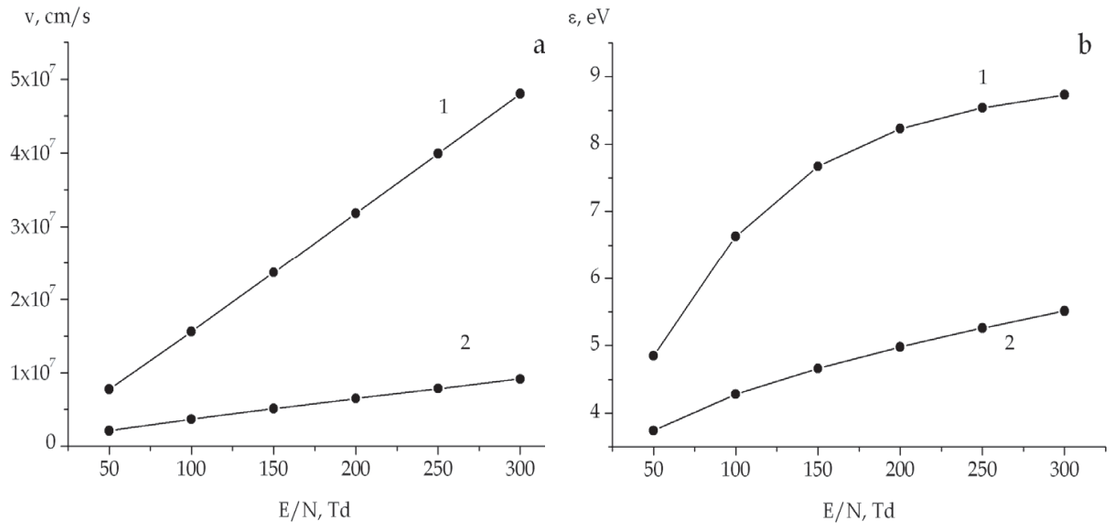

Fig. 3. Drift velocities (a) and mean energies (b) of electrons in the He:I_2-I= 800-50-50 Pa (1) and Xe:I_2-I= 800-50-50 Pa (2) mixtures as functions of the electric field in the discharge

The maximum electron drift velocities are also reached in the helium mixture and fall when passing to xenon. This fact is explained by a more intense electron scattering by xenon (the values of the momentum-transfer cross section for electron scattering by xenon atoms in the energy range 0-25 eV are one-two orders of magnitude higher than the corresponding characteristics of helium). The more intense electron scattering in xenon results in the decrease of the velocity of directed motion in this gas.

Tables 3-4 demonstrate the distribution of the power introduced into the discharge among the most important electron processes (Shuaibov et al., 2010b). They are the reactions of excitation and ionization of the rare gases, halogen atoms and molecules as well as dissociation and dissociative attachment of electrons to iodine molecules. The processes of stepwise ionization of the rare gases and iodine were neglected. It is explained by the facts that the concentrations of excited atoms and molecules strongly depend on the time and that their values are several orders of magnitude smaller than the concentrations of the primary components of the mixture (He, Xe, I_2, and I).

One can see that, due to very high excitation and ionization thresholds of helium atoms, the prevailing portion of the power in the He-I_2-I mixture is spent for reactions with participation of the halogen. Insignificant power costs for the process of electron attachment to iodine molecules are explained by the very low threshold energy of this process close to zero. An increase of the electric field results in the growth of the number of fast electrons and the rising role of the processes of ionization of iodine as well as excitation and ionization of helium.

In the xenon-based mixture, the portion of the power spent for excitation and ionization of the rare gas is much higher. The comparable thresholds of the processes with participation of xenon and iodine result in the fact that, at low electric fields, the power is distributed among them nearly equally. An increase of the electric field results in the growth of the portion of the power spent for processes with participation of the rare gas.

The highest rate is observed for the process with the smallest threshold (stepwise ionization of xenon), while the reactions with the lowest rates are those of helium and xenon ionization. The rates of all the processes grow with increasing electric field. The only

E/N, Td	He excitation	He ionization	I_2 excitation	I_2 attachment	I_2 dissociation	I_2 ionization	I excitation	I ionization
50	0.45	8.28e-5	12.9	9.56e-2	42	9.14	10	25.1
100	1.99	5.18e-4	7.6	3.01e-2	32	17	7.55	33
150	2.72	7.55e-4	6.37	2.08e-2	29	20	6.72	35
200	3.04	8.63e-4	5.92	1.79e-2	28	20.8	6.4	36
250	3.20	9.19e-4	5.71	1.66e-2	27	21.3	6.25	36
300	3.30	9.51e-4	5.6	1.59e-2	27	21.6	6.16	36

Table 3. Relative power costs for electron processes in the mixture He-I_2-I = 800-50-50 Pa (%)

E/N, Td	Xe excitation	Xe ionization	I_2 excitation	I_2 attachment	I_2 dissociation	I_2 ionization	I excitation	I ionization
50	58	0.163	17	0.44	17.6	1.12e-2	6.52	0.48
100	70	2.68	7.66	0.11	13.7	0.14	4.12	1.57
150	72	6.8	4.75	5.05e-2	10.7	0.33	3.0	2.22
200	71	10.8	3.38	2.88e-2	8.83	0.49	2.36	2.59
250	70,1	14.3	2.59	1.87e-2	7.52	0.65	1.95	2.80
300	68.6	17.3	2.09	1.31e-2	6.56	0.78	1.66	2.94

Table 4. Relative power costs for electron processes in the mixture Xe-I_2-I = 800-50-50 Pa (%)

exclusion is the dissociative attachment of electrons to iodine molecules that has the practically zero threshold and, correspondingly, does not depend on the number of fast electrons in the discharge.

The variation of the electric field in the range 50-300 Td results in the growth of the majority of the reaction rates within one order of magnitude. However, the helium ionization rate increases by four orders of magnitude owing to its strong dependence on the number of high-energy electrons.

The excitation and ionization rates of the rare gas in the xenon-iodine mixture are evidently higher than in the helium-iodine one due to lower threshold energies of these processes in xenon. As regards the reactions with participation of molecular and atomic iodine, their rates in the helium mixture are noticeably larger than in the xenon-based medium. It is explained by a much higher number of fast electrons in the discharge in helium that provide effective excitation, ionization, and dissociation of iodine.

Tables 5 and 6 present the values of the rates of the most important electron processes in the considered mixtures calculated as functions of the electric field in the discharge using Eq.(8) (Shuaibov et al., 2010b).

E/N, Td	50	100	150	200	250	300
He excitation	9.91e-13	1.36e-11	2.73e-11	3.6e-11	4.12e-11	4.44e-11
He ionization	1.62e-16	3.11e-15	6.66e-15	8.99e-15	1.04e-14	1.13e-14
I_2 excitation	1.77e-9	3.22e-9	3.97e-9	4.35e-9	4.56e-9	4.69e-9
I_2 attachment	6.71e-10	6.5e-10	6.61e-10	6.70e-10	6.76e-10	6.8e-10
I_2 dissociation	3.57e-9	8.45e-9	1.12e-8	1.26e-8	1.34e-8	1.39e-8
I_2 ionization	5.35e-10	3.09e-9	5.25e-9	6.51e-9	7.24e-9	7.7e-9
I excitation	1.08e-9	2.41e-9	3.16e-9	3.54e-9	3.76e-9	3.88e-9
I ionization	1.69e-9	6.9e-9	1.07e-8	1.29e-8	1.41e-8	1.49e-8

Table 5. Rates of electron processes in the mixture He-I_2-I= 800-50-50 Pa

E/N, Td	50	100	150	200	250	300
Xe excitation	7.42e-11	3.35e-10	7.33e-10	1.24e-9	1.84e-9	2.52e-9
Xe ionization	1.44e-13	8.81e-12	4.76e-11	1.29e-10	2.58e-10	4.37e-10
Xe stepwise ionization	2.3e-7	2.68e-7	2.92e-7	3.11e-7	3.26e-7	3.39e-7
I_2 excitation	2.30e-7	2.68e-7	2.92e-7	3.11e-7	3.26e-7	3.39e-7
I_2 attachment	7.51e-10	7.1e-10	6.84e-10	6.66e-10	6.52e-10	6.41e-10
I_2 dissociation	3.66e-10	1.05e-9	1.76e-9	2.47e-9	3.18e-9	3.88e-9
I_2 ionization	1.59e-13	7.61e-12	3.69e-11	9.54e-11	1.88e-10	3.17e-10
I excitation	1.65e-10	3.88e-10	6.01e-10	8.06e-10	1.0e-9	1.20e-9
I ionization	7.82e-12	9.54e-11	2.88e-10	5.72e-10	9.37e-10	1.37e-9

Table 6. Rates of electron processes in the mixture Xe-I_2-I= 800-50-50 Pa

3.2 Dependence of the emission intensities on the rare gas pressure

The analysis of the plasma kinetics in the mixture of rare gases with iodine vapours performed with regard for the described regularities makes it possible to study the effect of the buffer gas pressure on the emission intensities of molecular and atomic iodine. The results of the calculations performed for the helium-iodine mixture at the iodine concentration equal to 130 Pa are shown in Fig.4 (Shuaibov et al., 2010a).

One can see that the emission intensities of the 206-nm spectral line and the 342-nm molecular band of iodine depend on the helium pressure in the opposite ways. The emission intensity in the molecular band decreases with increasing rare gas pressure, while that in the 260-nm atomic line grows.

Excited iodine molecules $I_2(D')$ are generated in the discharge due to direct electron impact excitation. The rate of this process is determined by the electron energy distribution function and grows with increasing parameter *E/N*. Thus, an increase of the pressure of the mixture results in the decrease of the rate of formation of emitting $I_2(D')$ molecules in the discharge.

As was demonstrated in (Sauer, 1976; Baboshin, 1981), another important channel of generation of $I_2(D')$ molecules is the excitation transfer from the above-lying level $I_2(D)$ colliding with atoms and molecules of the active medium. However, at the considered pressures, the probability of radiation decay of the $I_2(D)$ state is much higher than the probability of its collision with other particles, that is why this channel makes practically no contribution to the formation of emitting $I_2(D')$ molecules.

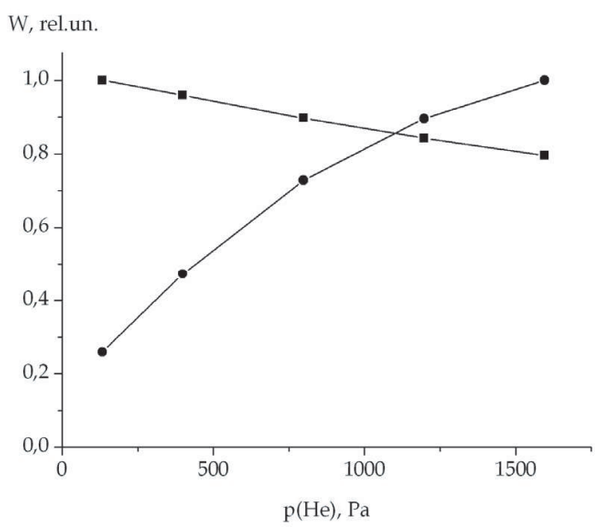

Fig. 4. Emission intensities of the 206-nm spectral line (●) and 342-nm molecular band (■) of iodine as functions of the helium pressure

A considerable part of iodine exists in the discharge in the dissociated state, which is confirmed by a high intensity of the 206-nm spectral line registered in a number of works (Avdeev, 2007; Shuaibov et al., 2005b; Zhang & Boyd, 2000). Measurements performed in (Barnes & Kushner, 1996, 1998) for Xe-I_2 mixture at pressures close to those used in our work have demonstrated that the fraction of iodine molecules dissociating in the discharge exceeds 90%. Moreover, the minimum concentration of I_2 molecules was registered at the axis of the discharge tube and the maximum one – close to the walls where iodine recovered to the molecular state.

Molecular iodine decays into atoms mainly owing to the processes of direct electron-impact dissociation (Table 1, reaction 8) and predissociation of the excited $I_2(B)$ state due to collisions with particles of the mixture (Table 1, reaction 12). The rate of the former reaction is determined by the form of the electron energy distribution function and decreases with increasing rare gas pressure, whereas the effectiveness of the latter process grows in direct proportion to the pressure.

Thus, an increase of the helium pressure in the He-I_2 glow discharge has a multiple effect on the efficiency of production of iodine atoms. The rate of electron-impact dissociation of the ground state of the iodine molecule falls due to the change of the electron energy distribution function. The rate of formation of the $I_2(B)$ excited state also decreases. At the same time, the efficiency of collisional predissociation of the $I_2(B)$ level abruptly increases, which appears determinative for the resulting effect.

Another important consequence of the increase of the rare gas pressure is the deceleration of the diffusion motion of iodine atoms to the walls of the discharge chamber, which results in the less efficient recovery of molecular iodine. Thus, with increasing pressure in the working medium of the halogen lamp, the relation between the concentrations of excited iodine molecules and atoms (and consequently powers of emission from the levels $I_2(D')$ and I^*) changes in favor of the latter.

3.3 Dependence of the emission intensities on the halogen pressure

With variation of the iodine concentration in the mixture, the emission intensities in the atomic 206-nm line and the 342-nm molecular band pass through a maximum (Fig.5). At $p(I_2) < 200$ Pa, the emission intensities grow with increasing halogen concentration, while at $p(I_2) > 200$-230 Pa, they sharply fall to zero.

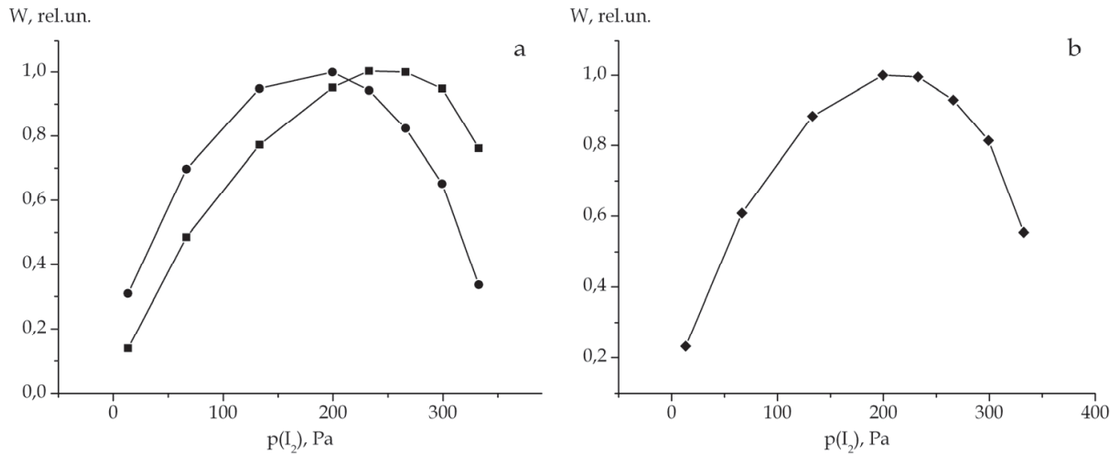

Fig. 5. Emission intensities of the spectral line of atomic iodine at 206 nm (●) and molecular band at 342 nm $I_2(D' \rightarrow A')$ (■) (a) and total emission intensity (b) as functions of the iodine concentration in the He-I_2 mixture at p(He)= 400 Pa

An increase of the iodine concentration is accompanied by the rise of the discharge voltage and reduction of the electron density in the discharge. This fact is caused by the effect of iodine on the electron energy distribution function. At low iodine concentrations, the distribution function is determined by the helium buffer gas characterized by large thresholds of excitation and ionization (19.8 eV and 22.5 eV, correspondingly). The addition of iodine to the active medium results in the cut-off of the distribution function at lower energies due to the smaller thresholds of its excitation and ionization as well as the increase of the total pressure of the mixture. Moreover, the rate of dissociative attachment of electrons to I_2 molecules (with a near-zero threshold) weakly depends on the iodine concentration, while the ionization rate determined by the tail of the distribution function sharply falls with increasing iodine content (Fig.6). The discharge voltage is determined by the balance of the ionization and attachment processes. That is why in order to maintain a discharge in a medium with a heightened halogen content, one should apply a larger voltage, which results in the decrease of the discharge current and, correspondingly, electron density.

The decrease of the electron concentration reduces the efficiency of generation of radiating particles in the discharge resulting in the decrease of the emission intensities both in the atomic line and in the molecular band of iodine. As one can see from Fig.5, the emission maximum in the case of the 342-nm band is reached at higher iodine pressure ≈ 230 Pa, whereas the emission intensity of atomic iodine starts falling already at $p(I_2)$ > 200 Pa. It is explained by the fact that the generation of excited iodine atoms is more sensitive to the electron density in the medium because it runs via two electron processes – electronic excitation of iodine molecules to the $I_2(B)$ level followed by decay into atoms (or direct electron-impact dissociation of molecular iodine) and consequent excitation of iodine atoms to the radiating level. Radiating $I_2(D')$ molecules are formed due to direct electronic excitation of molecular iodine. If the iodine concentration in the mixture exceeds 400 Pa, then the voltage falling across the discharge gap appears insufficient for the breakdown and the emission intensities abruptly fall to zero. The maximum of the summary emission intensity is reached at the iodine pressure equal to 200 Pa.

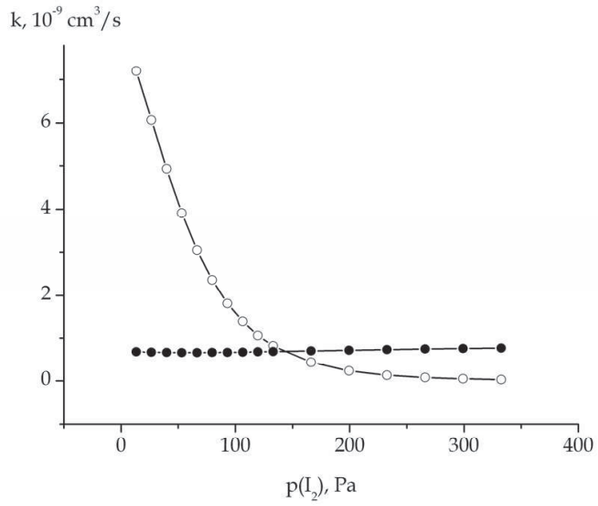

Fig. 6. Rates of dissociative attachment (●) and ionization (○) of iodine molecules as functions of the iodine concentration in the He-I_2 mixture at p(He)= 400 Pa and E = 150 V/cm

Taking into account the fact that the emission intensities of atomic and molecular iodine reach a maximum at different iodine concentrations, it is evident that the variation of its content in the mixture will result in the change of the relation between the emission intensities at 342 and 206 nm. With increasing iodine concentration, the relative emission intensity in the molecular band grows, and in the atomic line – falls. The calculated curve is given in Fig.7.

3.4 Effect of xenon on the emission of the excimer lamp

The presence of xenon in the active medium of the helium-iodine UV emitter results in the appearance of the additional emission band at 253 nm corresponding to the B→X transition of the XeI* excimer. As was already noted, XeI* molecules are generated in the discharge owing to the reverse harpoon reaction between a xenon atom in the ground state and some

highly excited level I_2** (Table 2, reaction 11). For today, the levels of molecular iodine participating in the reverse harpoon reaction are not identified. However, the analysis of the energy state diagram in the Xe:I_2:I mixture (Fig.1) testifies to the fact that neither of the states important for the kinetics in the helium-iodine medium has enough energy to excite the XeI* excimer molecule. It means that the addition of xenon does not result in the appearance of

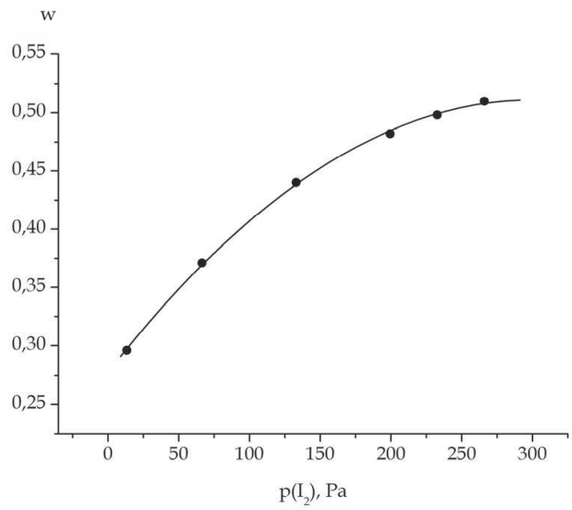

Fig. 7. Relative emission intensity in the 342-nm molecular band as a function of the iodine concentration in the He-I_2 mixture at p(He)= 400 Pa

additional channels of decay of the I_2(D') and I_2(B) states and influences their kinetics only through the electron distribution function. That is why, introducing a highly excited I_2** state with the minimum energy sufficient for the formation of the XeI* molecule and choosing its excitation cross section so that to provide the fraction of the emission intensity in the XeI*(B→X) band close to that observed experimentally, it is possible to analyze the effect of the xenon admixture on the emission intensities of atomic and molecular iodine.

The addition of xenon changes the plasma kinetics in three ways. The first one is the variation of the electron energy distribution function, namely, the decrease of the number of fast electrons in the discharge. The smaller number of high-energy electrons results in the reduction of the rates of the electron processes responsible for the formation of both excited atoms and molecules of iodine. However, the other two factors facilitate the generation of atomic iodine. One of them is the increase of the efficiency of decay of the excited I_2(B) level in its collisions with buffer gas atoms. The rate of this process in xenon is higher than in helium by a factor of 20. The second process is the decrease of the diffusion rate of iodine atoms to the walls of the discharge chamber due to the fact that the larger radius of xenon atoms as compared to helium ones provides the decrease of the mean free path of iodine atoms in the helium-xenon medium. These two factors result in the increase of the concentration of excited iodine atoms in the discharge.

According to the results of numerical simulations, the relation between the emission intensities of atomic and molecular iodine in He-I_2=400:130 Pa mixture amounts to W(206.2 nm)-W(342 nm) = 56-44%, whereas in the He-Xe-I_2=400:130:130 Pa medium, it changes to W(206.2 nm)-W(342 nm)=55:31%. Thus, the addition of xenon results in the decrease of the relative emission intensity of the 342-nm molecular band.

The dependences of the emission intensities on the concentration of iodine vapours in the mixture including xenon (p(He)-p(Xe) = 400-130 Pa) are qualitatively the same as those calculated for the He-I_2 medium. The maximum emission power in the 206-nm spectral line is reached at p(I_2)=230 Pa, while in the 342-nm band – at p(I_2)=170 Pa. Moreover, the maximum iodine concentration, at which the discharge is still initiated, is lower than in helium and amounts to 240 Pa. Such a difference is related to the fact that the ionization rates in the helium-iodine mixture at equal iodine concentration are lower than in the helium one, that is why the maintenance of the discharge requires higher voltages.

4. Comparison with experiment

The results of numerical simulations were compared to the data of experimental studies reported in a cycle of works (Shuaibov et al., 2004, 2005b, 2009).

A longitudinal glow discharge in helium and xenon rare gases was initiated in a cylindrical discharge tube made of quartz transparent to λ = 190 nm. The distance L between the cylindrical nickel electrodes was equal to 50 cm. The thickness of the tube walls and its inner diameter amounted to 1 mm and 1.4 cm, correspondingly. Crystalline iodine of high purity was located in a special appendix behind the anode of the discharge tube. The diagram of the experimental set-up is shown in Fig.8.

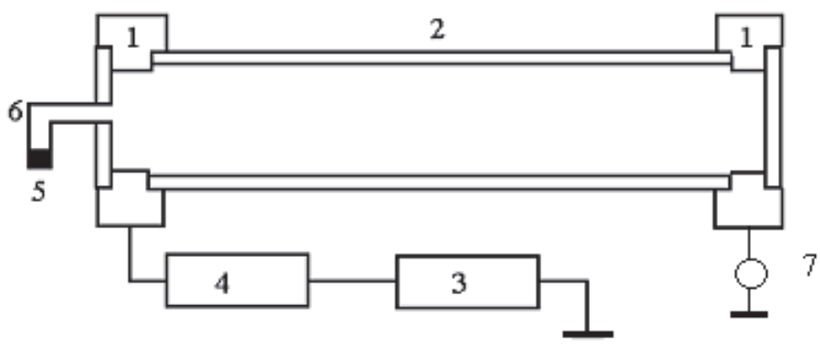

Fig. 8. Experimental set-up used for obtaining the glow discharge in mixtures of rare gases with iodine vapours: 1 - electrodes, 2 - quartz discharge tube, 3 - high-voltage rectifier, 4 - ballast resistor, 5 - iodine crystals, 6 - container for iodine, 7 - ammeter

The emission spectrum of the helium-iodine discharge included the spectral line of atomic iodine at 206 nm and a molecular band I_2 (D'-A') at 342 nm. At the partial helium pressure equal to 400 Pa, the emission intensities related as W(206.2 nm)-W(342nm) = 52-48 %. These values are in good agreement with the calculation results: W(206.2 nm)-W(342nm) = 56-44%.

The addition of xenon to the active medium of the UV emitter resulted in the appearance of the emission band at 253 nm, corresponding to the B→Xtransition of the XeI* molecule. At p(He)-p(Xe)=400-130 Pa, the emission intensities related as W(206.2 nm)-W(253 nm)-W(342 nm)=54-9-37%. In this case, the numerical computations yield the relation W(206.2 nm)-W(342 nm)=55:31%. Thus, both experimental and theoretical results testify to the fact that the addition of xenon to the active medium of the excimer lamp results in the decrease of the relative emission intensity of the I_2 (D'-A') molecular band, while that of the 206-nm line remains practically the same.

The experimentally obtained dependences of the registered emission intensities on the helium pressure in the He-I_2 mixture are presented in Fig.9. One can see that, with increasing helium pressure, the intensity of the molecular band decreases and that of the atomic line – grows. Such a behavior completely agrees with the results obtained by numerical simulation of the discharge kinetics in the UV emitter.

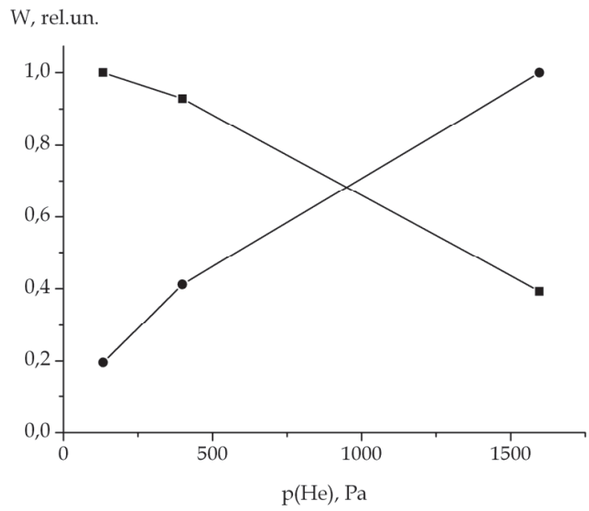

Fig. 9. Experimentally measured emission intensities of 206-nm spectral line (●) and 342-nm molecular band (■) of iodine as functions of the helium pressure

5. Conclusion

The numerical simulation of the discharge and emission kinetics in excimer lamps in mixtures of helium and xenon with iodine vapours allowed us to determine the most important kinetic reactions having a significant effect on the population kinetics of the emitting states in He:I_2 and He:Xe:I_2 mixtures. The opposite behavior of the dependences of the emission intensities of atomic and molecular iodine on the buffer gas pressure is explained. The influence of the halogen concentration on the emission power of the excimer lamp is investigated. The effect of xenon on the relative emission intensities of iodine atoms and molecules is analyzed. The calculation results are in good agreement with data of experimental studies, which is an evidence of the right choice of the calculation model and elementary processes for numerical simulation.

6. References

Avdeev, S.M.; Zvereva G.N., & Sosnin, E.A. (2007). Investigation of the conditions of efficient I^*_2 (342 nm) luminescence in a barrier discharge in a Kr-I2 mixture. *Optics and Spectroscopy*. Vol. 103, pp. 910-919

Baboshin, V.N., Mikheev, L.D., Pavlov, A.B., Fokanov, V.P., Khodorkovskii, M.A., & Shirokikh, A.P. (1981). Investigation of the luminescence and excitation spectrum of molecular iodine. *Soviet Journal of Quantum Electronics.* Vol. 11, pp. 683-686

Baginskii, V.M., Vladimirov, V.V., Golovinskii, P.M, & Shchedrin, A.I. (1988). *Optimization and stability of discharge in He/Xe/HCl excimer lasers*. Preprint of Acad. of Sci. of UkrSSR, Kyiv

Barnes P.N. & Kushner M.J. (1996). Formation of XeI(B) in low pressure inductive radio frequency electric discharges sustained in mixtures of Xe and I2. *Journal of Applied Physics*. Vol. 80, pp. 5593-5595

Barnes P.N. & Kushner M.J. (1998). Reactions in the afterglow of time modulated inductive discharges of Xe and I_2 mixtures. *Journal of Applied Physics*. Vol. 84, pp. 4727-4730

Boichenko, A.M. & Yakovlenko, S.I. (2003). Simulation of Xe/I2 Lamp Kinetics upon Capacitive Discharge Excitation. *Laser Physics*. Vol. 13, pp. 1461–1466

Cartwright, D.C., Csanak, G., Trajmar, S., & Register, D.F. (1992). Electron-impact excitation of the n1P levels of He. *Physical Review A* . Vol. 45, pp. 1602-1624

Golant, V.E., Zhilinsky A.P., & Sakharov I.E. (1980) *Fundamentals of Plasma Physics,* Wiley, ISBN 0-471-04593-4, New York

Hayashi, M. (2003) Bibliography of Electron and Photon Cross Sections with Atoms and Molecules Published in the 20th Century. Halogen Molecules, Available from: <www.nifs.ac.jp/report/NIFS-DATA-081.pdf>

Hyman, H.A. (1979). Electron-impact ionization cross sections for excited states of rare gases (Ne, Ar, Kr, Xe), cadmium, and mercury. *Physical Review A*. Vol. 20, pp. 855–859

Kireev, S.V. & Shnyrev, S.L. (1998). Collisional Predissociation of Vibrational Levels of the *B* state in I_2 Excited by 633-nm Radiation of a He–Ne Laser. *Laser Physics*. Vol. 8, pp. 483–486

Liuti G. & Mentall J.L. (1968). Monochromatic Iodine Lamp. *Review of Scientific Instruments*. Vol. 39, pp. 1767-1768

Lomaev, M.I., Skakun, V.S., Sosnin E.A., Tarasenko V.F., Shitts D.V., & Erofeev M.V. (2003). Excilamps: efficient sources of spontaneous UV and VUV radiation. *Physics-Uspekhi*, Vol. 46, pp. 193–209

Lomaev M.I. & Tarasenko V.F. (2002). Xe(He) I2-Glow and Capacitive Discharge Excilamps. *Proceedings of SPIE*. Vol. 4747, pp. 390-396

McDaniel, E.W. & Nighan, W.L. (Eds.). (1982). *Applied Atomic Collision Physics. Vol. 3. Gas Lasers*. Academic Press, ISBN 0-12-478803-3, New York

National Institute for Fusion Science. (n.d.). Xenon. Recommended electron collision cross sections, Available from: < dpc.nifs.ac.jp/DB/IEEJ/datafiles/Xe/Xe.pdf>

Raizer, Yu.P. (1991). *Gas Discharge Physics*, Springer, ISBN 978-3540194620, Berlin

Rejoub, R., Lindsay, B.G., & Stebbings, R.F. (2002). Determination of the absolute partial and total cross sections for electron-impact ionization of the rare gases. *Physical Review A*. Vol.65, 042713

Rhodes, C.K. (Ed.). (1984). *Excimer Lasers*, Springer-Verlag, ISBN 978-3540130130, Berlin

Saha, H.P. (1989). Accurate ab initio calculation on low-energy elastic scattering of electrons from helium. *Physical Review A*. Vol. 40, pp. 2976-2990

Sauer, M.C., Mulac, W.A., Cooper, R.F., & Grieser, F. (1976). Fast excited state formation and decay in the pulse radiolysis of gaseous argon–iodine systems. *Journal of Chemical Physics.* Vol. 64, pp. 4587-4591

Shuaibov, A.K. & Grabovaya, I.A. (2004). Electric-Discharge He/Xe/I2 excimer-halogen lamp. *Technical Physics*. Vol. 49, pp. 443-446

Shuaibov, A.K. & Grabovaya, I.A. (2005). A continuously emitting electric discharge UV lamp. *Instruments and Experimental Techniques*. Vol. 48, pp. 102-104

Shuaibov, A.K. & Grabovaya, I.A. (2005). Emission characteristics of a glow discharge in a mixture of heavy inert gases with iodine vapor. *Optics and Spectroscopy*. Vol. 98, pp. 510-513

Shuaibov, A.K., Minya, A.I., Gomoki, Z.T., Kalyuzhnaya, A.G. & Shchedrin, A.I. (2009). Output characteristics and parameters of the plasma from a gas-discharge low-pressure ultraviolet source on helium-iodine and xenon-iodine mixtures. *Technical Physics*. Vol. 54, pp. 1819-1824

Shuaibov, A.K., Gomoki, Z.T., Kalyuzhnaya, A.G. & Shchedrin, A.I. (2010). Radiative characteristics and kinetics of processes in low-pressure gas-discharge lamps on a mixture of helium and iodine vapors. *Optics and Spectroscopy*. Vol. 109, pp. 669-673

Shuaibov, A.K., Minya, A.I., Gomoki, Z.T., Kalyuzhnaya, A.G. & Shchedrin, A.I. (2010). Ultraviolet gas-discharge lamp on iodine molecules. *Technical Physics*. Vol. 55, pp. 1222-1225

Smirnov, B.M. (1967). *Atomic Collisions and Elementary Processes in Plasmas*, Atomizdat, Moscow

Soloshenko, I.A., Tsiolko, V.V., Pogulay, S.S., Terent'yeva, A.G., Bazhenov, V.Yu., Shchedrin, A.I., Ryabtsev, A.V., & Kuzmichev, A.I. (2007). The component content of active particles in a plasma-chemical reactor based on volume barrier discharge. *Plasma Sources Science and Technology*. Vol.16, pp. 56-66

Soloshenko, I.A., Tsiolko, V.V., Pogulay, S.S., Kalyuzhnaya, A.G., Bazhenov, V.Yu., & Shchedrin, A.I. (2009). Effect of water adding on kinetics of barrier discharge in air. *Plasma Sources Science and Technology*. Vol. 18, 045019

Stoilov, Yu. Yu. (1978). Characteristics of short-pulse iodine laser amplifier. *Soviet Journal of Quantum Electronics*. Vol. 8, pp. 223-226

Tam, Wing-Cheung & Wong, S.F. (1978). Dissociative attachment of halogen molecules by 0–8 eV electrons. *Journal of Chemical Physics*. Vol. 68, pp. 5626-5630

Zhang, J.-Y. & Boyd, I.W. (1998). Efficient XeI* excimer ultraviolet sources from a dielectric barrier discharge. *Journal of Applied Physics*. Vol. 84, pp. 1174-1178

Zhang, J.-Y. & Boyd, I.W. (2000). Multi-wavelength excimer ultraviolet sources from a mixture of krypton and iodine in a dielectric barrier discharge. *Applied Physics B*. Vol. 71, pp. 177-179

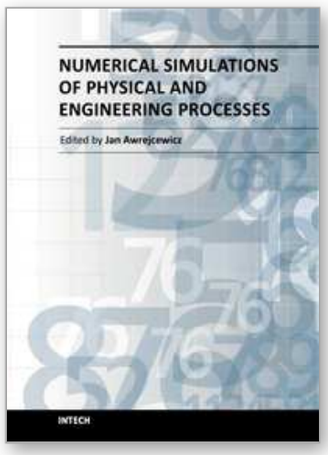

Numerical Simulations of Physical and Engineering Processes

Edited by Prof. Jan Awrejcewicz

ISBN 978-953-307-620-1
Hard cover, 594 pages
Publisher InTech
Published online 26, September, 2011
Published in print edition September, 2011

Numerical Simulations of Physical and Engineering Process is an edited book divided into two parts. Part I devoted to Physical Processes contains 14 chapters, whereas Part II titled Engineering Processes has 13 contributions. The book handles the recent research devoted to numerical simulations of physical and engineering systems. It can be treated as a bridge linking various numerical approaches of two closely inter-related branches of science, i.e. physics and engineering. Since the numerical simulations play a key role in both theoretical and application oriented research, professional reference books are highly needed by pure research scientists, applied mathematicians, engineers as well post-graduate students. In other words, it is expected that the book will serve as an effective tool in training the mentioned groups of researchers and beyond.

How to reference

In order to correctly reference this scholarly work, feel free to copy and paste the following:

Anatolii Shchedrin and Anna Kalyuzhnaya (2011). Numerical Simulation of Plasma Kinetics in Low-Pressure Discharge in Mixtures of Helium and Xenon with Iodine Vapours, Numerical Simulations of Physical and Engineering Processes, Prof. Jan Awrejcewicz (Ed.), ISBN: 978-953-307-620-1, InTech, Available from: http://www.intechopen.com/books/numerical-simulations-of-physical-and-engineering-processes/numerical-simulation-of-plasma-kinetics-in-low-pressure-discharge-in-mixtures-of-helium-and-xenon-wi

INTECH
open science | open minds

InTech Europe
University Campus STeP Ri
Slavka Krautzeka 83/A
51000 Rijeka, Croatia
Phone: +385 (51) 770 447
Fax: +385 (51) 686 166
www.intechopen.com

InTech China
Unit 405, Office Block, Hotel Equatorial Shanghai
No.65, Yan An Road (West), Shanghai, 200040, China
中国上海市延安西路65号上海国际贵都大饭店办公楼405单元
Phone: +86-21-62489820
Fax: +86-21-62489821

IntechOpen